Quickest Detection of Series Arc Faults on DC Microgrids

Kaushik Gajula, Vu Le, Xiu Yao, Shaofeng Zou, and Luis Herrera
Department of Electrical Engineering
University at Buffalo

2021 IEEE Energy Conversion Congress and Exposition (ECCE) | 978-1-7281-5135-9/21/$31.00 ©2021 IEEE | DOI: 10.1109/ECCE47101.2021.9595315

***Abstract*—In this paper we explore the problem of series arc fault detection and localization on dc microgrids. Through a statistical model of the microgrid obtained by nodal equation, the injection currents are modeled as a random vector whose distribution depends on the nodal voltages and the admittance matrix. A series arc fault causes a change in the admittance matrix, which further leads to a change in the data generating distribution of injection currents. The goal is to detect and localize faults on different lines in a timely fashion subject to false alarm constraints. The model is formulated as a quickest change detection problem, and the classical Cumulative Sum algorithm (CUSUM) is employed. The proposed framework is tested on a dc microgrid with active (constant power) loads. Furthermore, a case considering fault detection in the presence of an internal node is presented. Finally, we present an experimental result on a four node dc microgrid to verify the practical application of our approach.**

***Index Terms*—DC microgrid, Series arc fault detection and localization, Quickest change detection, CUSUM, Kron reduction**

I. Introduction

DC microgrids have seen a significant rise in deployment over the last decades. From solar, wind, hydro based power sources for electric utility, applications in Electric Vehicles (EVs), electric ships, More Electric Aircrafts (MEAs), to prospective applications in inter-planetary travel, etc. In consonance with the rise in dc microgrid's popularity and its advantages over the ac microgrid like efficiency, cost, and size, it is essential to find solutions for its drawbacks such as the Series Arc Faults (SAFs).

In recent years, different approaches have been proposed for SAF detection and localization. In [1], [2], SAF detection and localization was performed on a distribution node using Recursive Least Squares (RLS), Kalman Filter (KF) and gradient descent parameter estimation methods. SAF detection and localization was then analyzed on a dc microgrid by using KF as a parameter estimation algorithm in [3]. In the presence of limited number of sensors, a dual state and parameter estimation method which incorporates RLS and KF is presented in [4]. Machine learning based techniques studying the arc characteristics by collecting data, were presented in [5], [6]. A relative comparison of current variability in terms of frequency spectrum and time series is proposed in [7] for SAF detection. A time-domain technique based on the mathematical morphology called the decomposed open–close alternating sequence (DOCAS) is shown in [8] for SAF detection and localization. In [9], support vector machine optimized by particle swarm optimization (PSO-SVM) is designed to detect the arc fault.

In this paper, we propose to solve the SAF detection and localization on a dc microgrid [10]–[12] using the approach of Quickest Change Detection (QCD). In QCD problems, a stochastic system can be observed sequentially in time [13]–[15]. After a change occurs in the data generating distribution, the goal is to detect the change as quickly as possible subject to false alarm constraints. The approach of QCD has been applied for various fault and outage detection problems, including line outages and/or short circuit fault detection in ac systems [16], [17], line to line fault detection in circuits containing Photovoltaics (PVs) [18], and power system's outage detection in [19], [20]. These references model their networks using a generalized ac power flow. Application of modified-online CUSUM algorithm for quickest detection of false data injection attacks in microgrids is presented in [21]. The generalized CUSUM algorithm is employed for quickest detection of cyber-attacks in [22]. The adaptive CUSUM algorithm for defending false data injection attacks in smart grid networks is proposed in [23]. In [24], a novel backup protection algorithm based on QCD is proposed to offer fast and robust backup protection functionality for the primary relay.

In this paper, we analyze a dc microgrid as a static system using nodal analysis. We then formulate the SAF detection and localization as a QCD problem and investigate over two case studies: 1) generator and load at every node and 2) presence of internal node (s) in a dc microgrid. Our main contributions include: SAF detection and localization on a dc microgrid by using the CUSUM algorithm [25], and fault detection in a dc microgrid with internal nodes using Kron reduction. This paper is structured as follows: In section 2, a statistical model for the dc microgrid is developed. In section 3, the QCD based fault detection method is presented. Sections 4 and 5 present simulation and experimental results respectively. Finally, conclusion and future work are presented in section 6. The following notation is used in this paper: given a set $\mathcal{X}$, its cardinality is denoted by $|\mathcal{X}|$.

II. DC Microgrid

A classic dc microgrid is a power distribution system consisting of renewable source generators, Constant Power Loads (CPLs), Resistive Loads (RLs), energy storage devices, etc. A dc microgrid's topology can be defined as an undirected graph represented by $\mathcal{G} = (\mathcal{V}, \mathcal{E})$, where $\mathcal{V}$ is the set of

nodes/buses and $\mathcal{E} \subset \mathcal{V} \times \mathcal{V}$ is the set of edges/lines. The total number of nodes in $\mathcal{G}$ is $N = |\mathcal{V}|$ and each line/edge in the dc network is defined as $(m, n) \in \mathcal{E}$, where $m, n \in \mathcal{V}$.

The nodal equation for a dc network at a sampling instant $k \in \mathbb{Z}_{\geq 0}$ is given by

$$I[k] = YV[k], \tag{1}$$

where $I \in \mathbb{R}^N$ denotes the current injection at each node $i \in \mathcal{V}$, $V \in \mathbb{R}^N$ denotes the nodal voltages, and admittance matrix is denoted by $Y \in \mathbb{R}^{N \times N}$. Considering the difference along consecutive samples of $I[k]$ and $V[k]$, we define

$$\begin{aligned} \Delta I[k] &= I[k] - I[k-1], \\ \Delta V[k] &= V[k] - V[k-1]. \end{aligned} \tag{2}$$

The nodal equation (1) then becomes:

$$\Delta I[k] = Y \Delta V[k]. \tag{3}$$

In the above equation, $\Delta V[k]$ is defined to be independent and identically distributed Gaussian random variable which can be denoted by:

$$\Delta V[k] \sim \mathcal{N}(0,\ \Upsilon). \tag{4}$$

Consequently, we define $\Delta I[k]$ as

$$\Delta I[k] \sim \mathcal{N}(0,\ \Sigma_0), \tag{5}$$

where $\Sigma_0 = Y \Upsilon Y^T$ is the covariance matrix. The pre-fault probability distribution function (pdf) of the current difference $\Delta I[k]$ is denoted by f_0.

III. Series Arc Fault

A SAF can be defined as a power discharge in series with the circuit. It is a consequence of wear and tear or line breakage. On transfer of charge through an air gap in series, energy is dissipated in the form of heat and light (fire) which can cause major damage to a system and might also lead to fatalities in EVs, MEAs, electric ships, etc. Fig. 1 depicts a SAF on a line (m, n) where $r_{(m,n)}$ is the pre-fault line resistance, and $r_{(m,n)SAF}$ is the arc resistance. When a SAF is triggered the total line resistance of the line (m, n) becomes

$$r_{(m,n)\gamma} = r_{(m,n)} + r_{(m,n)SAF}. \tag{6}$$

We then define the new line conductance as

$$y_{(m,n)\gamma} = \frac{1}{r_{(m,n)} + r_{(m,n)SAF}}. \tag{7}$$

Assuming that there is a fault at line (m, n), we define the matrix $Y_{(m,n)}$ such that all $y_{(m,n)}$ are replaced with $y_{(m,n)\gamma}$, where $y_{(m,n)}$ is the pre-fault line admittance. The nodal characteristics during a fault at this line can be represented by

$$\Delta I[k] = Y_{(m,n)} \Delta V[k]. \tag{8}$$

While the covariance of $\Delta V[k]$ remains Υ, the covariance of $\Delta I[k]$ changes to

$$\Delta I[k] \sim \mathcal{N}(0,\ \Sigma_{(m,n)}), \tag{9}$$

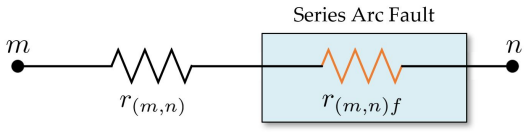

Fig. 1. Series arc fault model considered on line (m, n).

where the new covariance is given by

$$\Sigma_{(m,n)} = Y_{(m,n)} \Upsilon Y_{(m,n)}^T. \tag{10}$$

IV. Quickest Change Detection

In this section we present the CUSUM algorithm and the Kron reduction based internal node elimination.

A. Current sensors at all nodes

The objective of the CUSUM algorithm is to minimize the detection delay when the distribution of $I[k]$ changes from f_0 to $f_{(m,n)}$ subject to false alarm constraints. This problem can be formulated as [26]:

$$\begin{aligned} &\min_{\tau} \sup_{\gamma > 0} E_\gamma \left[\tau - \gamma \mid \tau \geq \gamma \right] \\ &\text{subject to } E_\infty \left[\tau \right] \geq \beta. \end{aligned} \tag{11}$$

where τ is defined as the stopping time, and the change point at which an event occurs is given by γ. The expectation of an event to occur at time γ is given by E_γ, the expectation when there is no fault is given by E_∞ and β is the desired mean time to false alarm.

The CUSUM detection statistic for a SAF on line (m, n) is updated as follows:

$$W_{(m,n)}[k+1] = \left(W_{(m,n)}[k] + \log \frac{f_{(m,n)}\left(\Delta I[k+1]\right)}{f_0\left(\Delta I[k+1]\right)} \right)^+, \tag{12}$$

where f_0 and $f_{(m,n)}$ define the pre and post-fault pdfs of the dc microgrid when there is a SAF on line (m, n). The algorithm is initiated with $W_{(m,n)}[0] = 0$ and $(\cdot)^+ = \max\{0, \cdot\}$. Finally, a fault is said declared whenever the detection statistics $W_{(m,n)}[k]$ on any line (m, n) exceeds a pre-specified threshold A_{td}, and the stopping time is defined as follows:

$$\tau = \inf_{k \geq 0} \left\{ k : \Big| \max_{(m,n) \in \mathcal{E}} W_{(m,n)}[k] \geq A_{td} \right\}, \tag{13}$$

where the threshold A_{td} can be computed as in [13], [16] to meet the false alarm constraints:

$$A_{td} = \log\left(|\mathcal{E}|\beta\right). \tag{14}$$

To further localize the SAF, the line whose detection statistic exceeds the threshold at the stopping time is then claimed to have a SAF:

$$\arg\max_{(m,n) \in \mathcal{E}} W_{(m,n)}[\tau] \tag{15}$$

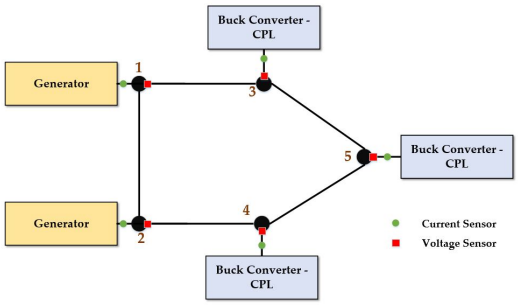

(a) Case 1 simulation results.

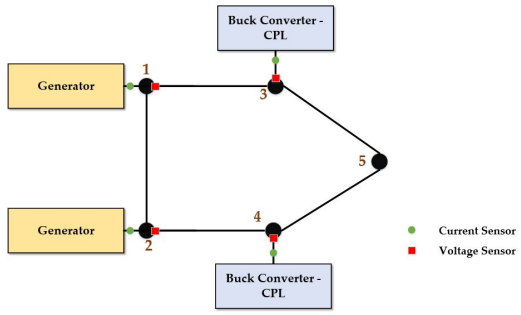

(b) Case 2 simulation results.

Fig. 2. Dc microgrid model for the two cases.

B. Internal Node Elimination

In this section we present an alternative formulation by Kron reduction approach to detect a SAF when there are internal nodes present in the dc microgrid.

Let $\alpha \subseteq \mathcal{V}$ be the set of nodes such that a generator and/or load is connected to each element and $\beta \subset \mathcal{V}$ be the internal nodes with no generator or load connection. The set of nodes is then decomposed as $\mathcal{V} = \alpha \cup \beta$. We can then rewrite equation (3) as

$$\begin{pmatrix} \Delta I_\alpha \\ 0_\beta \end{pmatrix} = \begin{pmatrix} Y_{\alpha,\alpha} & Y_{\alpha,\beta} \\ Y_{\beta,\alpha} & Y_{\beta,\beta} \end{pmatrix} \begin{pmatrix} \Delta V_\alpha \\ \Delta V_\beta \end{pmatrix}, \tag{16}$$

where ΔI_α is current injection measurement and ΔV_α is the nodal voltage measurement at the nodes in α. Similarly, ΔV_β is the nodal voltage measurement at β and 0_β is a column vector of zeros (internal nodes). Therefore,

$$0_\beta = Y_{\beta,\alpha}\Delta V_\alpha + Y_{\beta,\beta}\Delta V_\beta. \tag{17}$$

We can solve for ΔV_β:

$$\Delta V_\beta = -\left[Y_{\beta,\beta}\right]^{-1} Y_{\beta,\alpha}\Delta V_\alpha. \tag{18}$$

Substituting ΔV_β on (16) we obtain

$$\begin{aligned} \Delta I_\alpha &= Y_{\alpha,\alpha}\Delta V_\alpha - Y_{\alpha,\beta}\left(\left[Y_{\beta,\beta}\right]^{-1} Y_{\beta,\alpha}\Delta V_\alpha\right) \\ \implies \Delta I_\alpha &= \left(Y_{\alpha,\alpha} - Y_{\alpha,\beta}\left[Y_{\beta,\beta}\right]^{-1} Y_{\beta,\alpha}\right)\Delta V_\alpha. \end{aligned} \tag{19}$$

The above equation is of the form,

$$\Delta I_\alpha = \tilde{Y}\Delta V_\alpha. \tag{20}$$

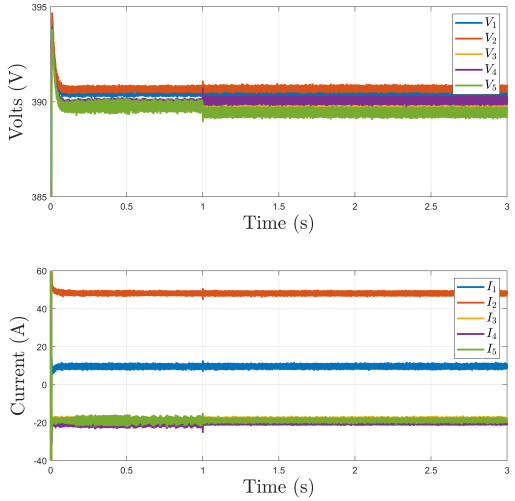

(a) Case 1: Node voltages (top) and current injections (bottom) for system without internal nodes.

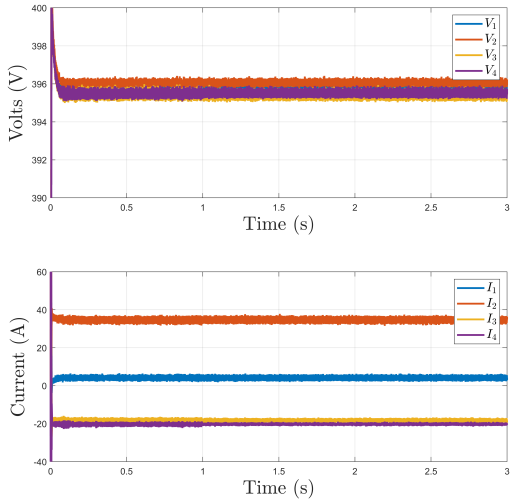

(b) Case 2: Node voltages (top) and current injections (bottom) for network with one internal node.

Fig. 3. Nodal voltages and injection currents for simulation results.

where $\tilde{Y}$ is the fault free admittance matrix. It can be shown that the reduced matrix $\tilde{Y}$ is a Laplacian of the sub-graph defined by the nodes α [27].

We can now similarly define a new reduced admittance matrix $\tilde{Y}_{(m,n)}$ associated with a SAF at each line $(m,n) \in \mathcal{E}$. Similarly, the post fault pdf $f_{(m,n)}$ of the current injections will be derived using the respective reduce admittance matrix and the QCD based CUSUM algorithm for SAF detection and localization can be applied.

V. Simulation Results

In this section, we present two case studies using the 5 node dc microgrid shown in Fig. 2. The nodal voltages and injection

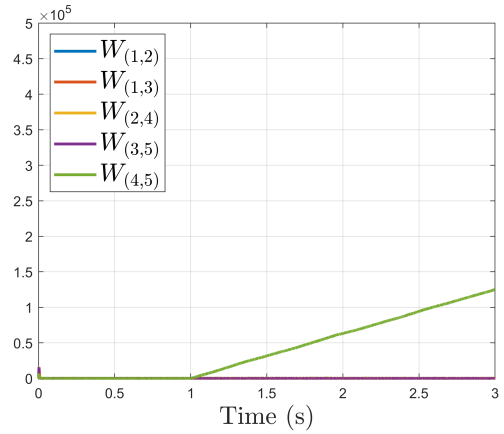

(a) Fault detection on line (4,5).

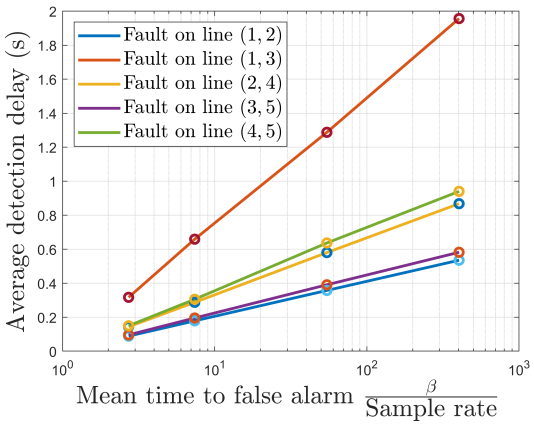

(b) Mean time to false alarm vs average detection delay .

Fig. 4. Case 1: Current sensors at all nodes.

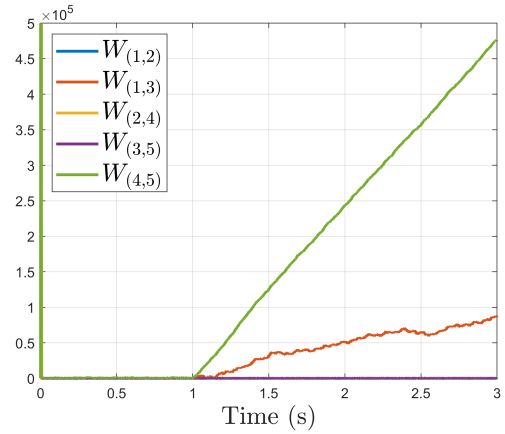

(a) Fault detection on line (4,5).

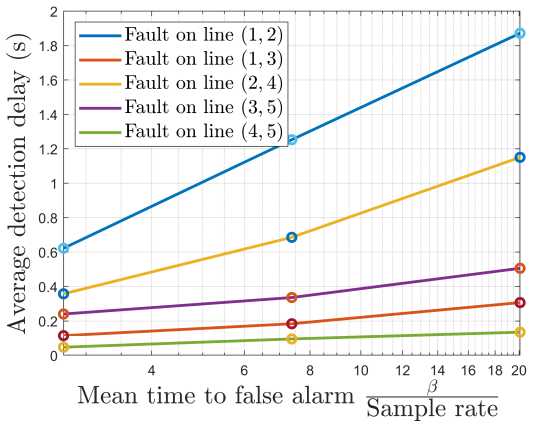

(b) Mean time to false alarm vs average detection delay .

Fig. 5. Case 2: Current sensor absent at node 5 (Internal node).

currents are presented in Fig. 3. In case 1, we present a CPL based model using closed loop control buck converters and in case 2, the same model is tested with Kron reduction approach when the injection current is zero at a node 5 (internal node). The simulation results were obtained by MATLAB and the sample time was set at 10 μs. The dc microgrid's parameters used for both the cases are tabulated in Table I. Both the case studies have their respective SAFs triggered at t = 1 s.

TABLE I. DC microgrid simulation parameters.

Line	**Length** (miles)	**Inductance** (mH)	**Resistance** **(mΩ)**
$(1,2)$	0.01	0.016	12
$(1,3)$	0.02	0.032	24
$(2,4)$	0.022	0.0352	26.4
$(3,5)$	0.008	0.0128	9.6
(4,5)	0.007	0.0112	8.4

A. *Case 1*

In this case, the microgrid shown in Fig. 2a is used. Two generators are connected at nodes 1 and 2. The CPL loads are connected at nodes 3, 4, and 5. Nodal voltages and injection currents of the microgrid are presented in Fig. 3a. The SAF on line $(4,5)$ was triggered at time t = 1 s. Fig. 4a shows SAF detection and localization on line $(4,5)$. When $W_{(4,5)}[k]$, denoted by the green line, crosses a certain threshold the fault on line $(4,5)$ is detected and localized. The mean time to false alarm vs the detection delay plot is presented in Fig. 4b which helps us understand that line $(1,3)$ has the maximum average detection delay, while line $(1,2)$ has minimum average detection delay given the same mean time to false alarm.

B. *Case 2*

The microgrid shown in Fig. 2b which includes two generators each at nodes 1 and 2 and two loads at nodes 3 and 4 was simulated. In this case, we consider node 5 as an internal node and its current and voltage sensor is not taken into consideration. Fig. 3b presents nodal voltages and injection currents of the microgrid. As can be seen in Fig. 5a, the SAF

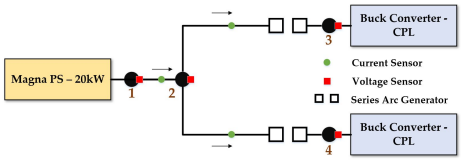

(a) Microgrid layout.

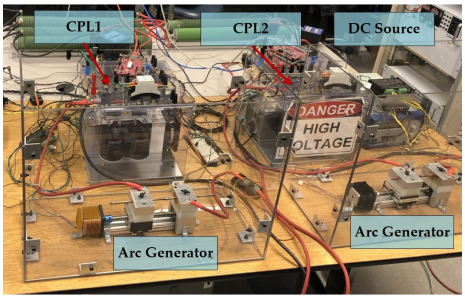

(b) Hardware components of the dc microgrid test-bed.

Fig. 6. Dc microgrid setup for experimental results.

was triggered at time t = 1 s on line $(4, 5)$. Due to the lack of measurements from the internal node (also the node connected to the faulted line), we do not see any disturbance in Fig. 3b when the fault occurs. The fault on line $(4, 5)$ is said to be successfully detected and localized when $W_{(4,5)}[k]$ crosses a fixed threshold. The mean time to false alarm vs the detection delay plot in Fig. 5b shows that after removing the load at node 5, line $(1, 2)$ has maximum average detection delay while line $(4, 5)$ has minimum average detection delay given the same mean time to false alarm.

VI. Experimental Results

The 4 node microgrid shown in Fig. 6 is used for experimental results. The microgrid includes Magna Power 20 kW as a generator at node 1 and two closed loop controlled buck converters as CPLs at nodes 3 and 4. The dc bus voltage was measured at 270 V while the current input by the loads at nodes 3 and 4 were set to 15 A and 10 A respectively. The voltage and current plots of the dc microgrid test-bed are presented in Fig. 7a. The SAF was triggered on line $(2, 3)$ at time t = 2.34 s. Fig. 7b presents the plot of $W_{(m,n)}[k]$ through which we can conclude that the fault is successfully detected and localized on line $(2, 3)$ once it crosses a certain fixed threshold A_{td}.

VII. Conclusion and Future Work

In this paper we present a QCD based algorithm for SAF detection on a dc microgrid with and without internal nodes. The SAF detection and localization was tested on a 5 node dc microgrid over two cases: a microgrid with either a generator or a load at each node and a microgrid with an internal node. The QCD based algorithm was further tested on a 4 node dc microgrid test-bed, where an internal node was established. Through the simulation and experimental results, it can be seen that the QCD based algorithm is a viable approach for SAF detection and localization.

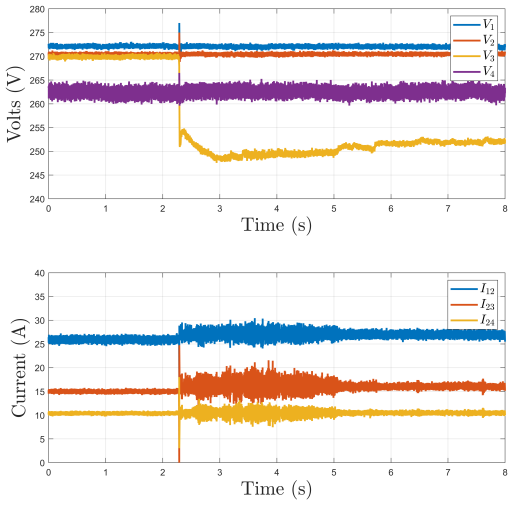

(a) Nodal voltages and nodal currents.

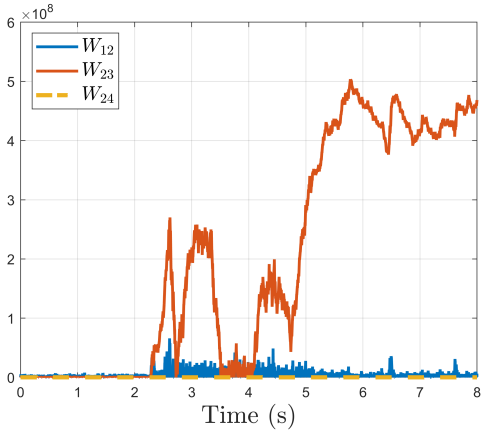

(b) Fault detection on line $(2, 3)$.

Fig. 7. Experimental results - SAF triggered at t = 2.34 s on line $(2, 3)$.

In the future, sensor placement techniques will be explored for a dc microgrid to enhance the line observability for the CUSUM algorithm when there is a shortage of sensors being deployed on a microgrid.

Acknowledgment

This material is based upon work supported by the National Science Foundation under Grants No. 1855888, No.1948165 and No. 1809839.

References

[1] K. K. Gajula, L. Herrera, and X. Yao, "Detection of series dc arc on a distribution node using discrete-time parameter identification techniques," in *2019 IEEE Applied Power Electronics Conference and Exposition (APEC)*, March 2019, pp. 3007–3012.

[2] L. Herrera and X. Yao, "Parameter identification approach to series dc arc fault detection and localization," in *2018 IEEE Energy Conversion Congress and Exposition (ECCE)*, Sep. 2018, pp. 497–501.

[3] K. Gajula and L. Herrera, "Detection and localization of series arc faults in dc microgrids using kalman filter," *IEEE Journal of Emerging and Selected Topics in Power Electronics*, 2020.

[4] K. Gajula, X. Yao, and L. Herrera, "Dual state-parameter estimation for series arc fault detection on a dc microgrid," in *2020 IEEE Energy Conversion Congress and Exposition (ECCE)*. IEEE, 2020, pp. 4649–4655.

[5] V. Le, X. Yao, C. Miller, and B.-H. Tsao, "Series dc arc fault detection based on ensemble machine learning," *IEEE Transactions on Power Electronics*, vol. 35, no. 8, pp. 7826–7839, 2020.

[6] V. Le and X. Yao, "Ensemble machine learning based adaptive arc fault detection for dc distribution systems," in *2019 IEEE Applied Power Electronics Conference and Exposition (APEC)*. IEEE, 2019, pp. 1984–1989.

[7] H.-P. Park and S. Chae, "Dc series arc fault detection algorithm for distributed energy resources using arc fault impedance modeling," *IEEE Access*, vol. 8, pp. 179 039–179 046, 2020.

[8] M. Kavi, Y. Mishra, and M. Vilathgamuwa, "Dc arc fault detection for grid-connected large-scale photovoltaic systems," *IEEE Journal of Photovoltaics*, vol. 10, no. 5, pp. 1489–1502, 2020.

[9] N. Qu, J. Zuo, J. Chen, and Z. Li, "Series arc fault detection of indoor power distribution system based on lvq-nn and pso-svm," *IEEE Access*, vol. 7, pp. 184 020–184 028, 2019.

[10] X. Yao, L. Herrera, S. Ji, K. Zou, and J. Wang, "Characteristic study and time-domain discrete- wavelet-transform based hybrid detection of series dc arc faults," *IEEE Transactions on Power Electronics*, vol. 29, no. 6, pp. 3103–3115, 2014.

[11] X. Yao, "Study on dc arc faults in ring-bus dc microgrids with constant power loads," in *Proceedings of the IEEE Energy Conversion Congress and Exposition (ECCE)*, 2016, pp. 1–5.

[12] X. Yao, L. Herrera, S. Ji, K. Zou, and J. Wang, "Characteristic study and time-domain discrete- wavelet-transform based hybrid detection of series dc arc faults," *IEEE Transactions on Power Electronics*, vol. 29, no. 6, pp. 3103–3115, 2014.

[13] V. V. Veeravalli and T. Banerjee, "Quickest change detection," in *Academic press library in signal processing*. Elsevier, 2014, vol. 3, pp. 209–255.

[14] H. V. Poor and O. Hadjiliadis, *Quickest Detection*. Cambridge University Press, 2008.

[15] A. Tartakovsky, I. Nikiforov, and M. Basseville, *Sequential analysis: Hypothesis testing and changepoint detection*. CRC Press, 2014.

[16] Y. C. Chen, T. Banerjee, A. D. Dominguez-Garcia, and V. V. Veeravalli, "Quickest line outage detection and identification," *Proceedings of the IEEE Transactions on Power Systems*, vol. 31, no. 1, pp. 749–758, 2015.

[17] T. Christman, N. Uhrich, P. Swisher, and X. Jiang, "A statistical approach for line outage detection in power systems with transient dynamics," in *IEEE International Conference on Probabilistic Methods Applied to Power Systems (PMAPS)*, 2018, pp. 1–5.

[18] L. Chen, S. Li, and X. Wang, "Quickest fault detection in photovoltaic systems," *Proceedings of the IEEE Transactions on Smart Grid*, vol. 9, no. 3, pp. 1835–1847, 2016.

[19] G. Rovatsos, X. Jiang, A. D. Domínguez-García, and V. V. Veeravalli, "Comparison of statistical algorithms for power system line outage detection," in *IEEE International Conference on Acoustics, Speech and Signal Processing (ICASSP)*, 2016, pp. 2946–2950.

[20] G. Rovatsos, X. Jiang, A. D. Domínguez-García, and V. V. Veeravalli, "Statistical power system line outage detection under transient dynamics," *IEEE Transactions on Signal Processing*, vol. 65, no. 11, pp. 2787–2797, 2017.

[21] B. Jin, C. Dou, and D. Wu, "False data injection attacks and detection on electricity markets with partial information in a micro-grid-based smart grid system," *International Transactions on Electrical Energy Systems*, vol. 30, no. 12, p. e12661, 2020.

[22] M. N. Kurt, Y. Yılmaz, and X. Wang, "Distributed quickest detection of cyber-attacks in smart grid," *IEEE Transactions on Information Forensics and Security*, vol. 13, no. 8, pp. 2015–2030, 2018.

[23] Y. Huang, J. Tang, Y. Cheng, H. Li, K. A. Campbell, and Z. Han, "Real-time detection of false data injection in smart grid networks: An adaptive cusum method and analysis," *IEEE Systems Journal*, vol. 10, no. 2, pp. 532–543, 2014.

[24] J. Sun, M. Saeedifard, and A. S. Meliopoulos, "Backup protection of multi-terminal hvdc grids based on quickest change detection," *IEEE Transactions on Power Delivery*, vol. 34, no. 1, pp. 177–187, 2018.

[25] E. S. Page, "Continuous inspection schemes," *Biometrika*, vol. 41, pp. 100–115, Jun. 1954.

[26] M. Pollak, "Optimal detection of a change in distribution," *The Annals of Statistics*, pp. 206–227, 1985.

[27] F. Dorfler and F. Bullo, "Kron reduction of graphs with applications to electrical networks," *IEEE Transactions on Circuits and Systems I: Regular Papers*, vol. 60, no. 1, pp. 150–163, 2013.